

Received December 14, 2020, accepted January 7, 2021, date of publication January 26, 2021, date of current version March 3, 2021.

Digital Object Identifier 10.1109/ACCESS.2021.3054616

# D2D Communication Underlying Microwave and Millimeter-Wave Cellular Networks Using CIPC

JAIR SEBASTIAN-VILLA<sup>1</sup> AND DOMINGO LARA-RODRÍGUEZ<sup>1</sup>

Center for Research and Advanced Studies, Department of Electrical Engineering, Communications Section, National Polytechnic Institute of Mexico (IPN), Mexico City 07300, México

Corresponding author: Domingo Lara-Rodríguez (dlara@cinvestav.mx)

**ABSTRACT** D2D communication is one of the promising technologies to improve network performance through direct wireless communication between users, without, or with limited participation of the base station (BS). In this paper, we investigate the performance of D2D communication underlying microwave ( $\mu$ -wave) and millimeter-wave (mm-wave) cellular networks using stochastic geometry. Rayleigh fading is considered to characterize the  $\mu$ -wave channels in both links, while the Rician fading is used to characterize the mm-wave channel in the D2D and cellular desired link. The D2D communication is established when the losses between the D2D transmitter and the D2D receiver are lower compared to the losses that exist between the D2D transmitter and the BS receiver. On the other hand, to minimize the interference caused by the coexistence of cellular and D2D communication and increase network performance, the Channel Inversion-Based Power Control (CIPC) is studied. In this way, the Complementary Cumulative Distribution Function (CCDF) for the successful transmission is obtained. Based on the analytical and numerical results, we show an important increase in the probability of successful transmission using the CIPC and considering the channel gains condition to establish the D2D communication compared to the traditional mode in which power control is not used and no conditions are considered to establish the D2D communication.

**INDEX TERMS** 5G, device-to-device (D2D) communication, microwave cellular networks, millimeter-wave cellular networks, Poisson point process, power control, Rayleigh fading, Rician fading, stochastic geometry.

## I. INTRODUCTION

The challenges for 5G and beyond wireless communications lie in achieving ultra-low latency, ultra-high reliability, high data-rate connectivity (on the order of Gbps), resource allocation and multiple access, quality latency-rate tradeoff, high number of connected devices, high efficient, energy efficiency, among others [1], [2]. With the 5G networks implementation new applications are also emerging, such as Device-to-Device (D2D) communication, Internet of Things (IoT), Machine-to-Machine communication (M2M), Internet of Vehicles (IoV), among others [3]. As one of the key technologies, D2D communication increases the network performance in terms of Spectral Efficiency (SE) and Energy Efficiency (EE), in addition to reducing transmission and retransmission delay, traffic and computation offloading [4], transmission power and alleviate congestion of cellular networks. D2D communication enables wireless transmission

between users over the direct link without, or with limited, participation of the BS or core network.

D2D communications is classified into inband D2D communication, where the communication takes place in the licensed cellular spectrum, providing SE due to the sharing of licensed spectrum between D2D and cellular users, and outband D2D communication where the communication takes place in the unlicensed spectrum [5]. In addition, inband D2D is classified into underlay and overlay mode. In overlay mode, dedicated spectrum is allocated to D2D communication, cellular users (CUs) and D2D users (DUs) use orthogonal channels. In underlay mode, D2D communication reuses the same spectrum, increasing the SE [6]. Nevertheless, the underlay mode becomes a new source of interference. As a result, cellular links experience interference from the D2D transmitters, and in spite of potential gains that this mode offers, the coexistence of D2D and cellular communication in the same spectrum creates technical challenges, among them, the interference management in the network. At present, power control techniques have been used

The associate editor coordinating the review of this manuscript and approving it for publication was Miguel López-Benítez<sup>1</sup>.

as a way to coordinate and mitigate the interference for D2D communications [7].

On the other hand, given the current shortage of the microwave spectrum, the key essence of 5G wireless networks and beyond lies in exploring the high frequency millimeter-wave band. Even a small fraction of available mm-wave spectrum can support hundreds of times of more data rate and capacity over the current cellular spectrum. Thus, due the abundance of unoccupied bandwidth available, the mm-wave band is a potential solution to resolve the spectrum crunch crisis and satisfy the requirements of 5G and beyond mobile communications [8]. However, mm-wave signal propagation is fundamentally different from that in traditional microwave band, and the propagation characteristics at these bands have a fundamental impact on each aspect of the cellular architecture, ranging from equipment design to real-time performance in the field [9]. Hence, careful design and consideration are necessary to ensure mm-wave cellular networks can really fulfill their great potential.

Therefore, characterizing the performance of power control for D2D underlying microwave and millimeter-wave cellular network is highly important for 5G wireless, and this problem is the main motivation of this paper.

The main contributions of this paper are summarized as follows:

1) We develop an analytical framework to analyze the uplink performance for the D2D communication underlying microwave and millimeter-wave cellular networks by using stochastic geometry. The cellular and D2D users random positions are spatially distributed as homogeneous Poisson point processes. Two environments are considered to analyze the uplink performance for the D2D communication underlying cellular network. First, the conventional microwave cellular environment. In this case, it is assumed that the multipath fading follows a Rayleigh model. Second, the mm-wave environment. For this case, it is assumed that the multipath fading follows a Rician fading model with  $K$ -factor for the desired signal, appropriate for each channel.

2) We propose a channel gain-based condition to establish the D2D link, where the D2D communication is carried out considering the channel gain between transmitter and receiver to establish the D2D link. In this way, the D2D link is studied considering that the losses between the D2D transmitter and the D2D receiver are lower compared to the losses that exist between the D2D transmitter and the BS, so that the D2D communication is more adequate in comparison with the normal cellular mode, increasing the performance of the network. Also, we assume the channel inversion-based power control as a strategy to mitigate the intra-cell interference introduced by the cellular and D2D users coexistence.

3) Using stochastic geometry tools, we obtain the successful transmission probability for cellular and D2D links in both microwave and millimeter-wave environments. First, we derive the general expressions and then, based on high SIR approximation, the closed-form expressions for specific path-loss values are derived. Furthermore, the distance

distributions between users are derived as an additional result to obtain these probabilities. Different simulations are performed to validated analytical results obtained for our proposed model.

4) Through the analytical and numerical results obtained under the model studied in this paper, we show that the channel gain-based condition to establish the D2D link together with CIPC provides a significant improvement in the successful transmission probability for cellular and D2D links in both microwave and millimeter-wave environments. Furthermore, we observe that the mm-wave environment presents better performance on the network compared to the microwave environment, given the dominant path conditions presented in the mm-wave environment under Rician fading.

The rest of the paper is organized as follows. The related work is reviewed in Section II. In Section III, we present the system model, the assumptions, the channel models for microwave and mm-wave cellular environment, and the power control technique implemented. In Section IV, we analyze the successful transmission probability in our proposed mode selection strategy, for the different environments. Section V presents and discusses the numerical and simulation results. Finally, the paper is concluded in Section VI. A summary of the notation used in this paper is given in Table 1.

TABLE 1. Notation summary.

Notation	Description
$\Phi_c$	PPP of Cellular users
$\lambda_c$	Density of Cellular users
$P_c$	Microwave cellular transmit power
$\bar{P}_c$	Millimeter-wave cellular transmit power
$K_c$	Cellular Rician factor
$\Phi_d$	PPP of D2D users
$\lambda_d$	Density of D2D users
$P_d$	Microwave D2D transmit power
$\bar{P}_d$	Millimeter-wave D2D transmit power
$K_d$	D2D Rician factor
$P_{min}$	Receiver sensitivity
$\alpha$	Microwave path loss exponent
$\beta$	Millimeter-wave path loss exponent
$T$	SIR threshold
$\mathcal{P}_c^\mu$	Microwave Successful transmission probability CU's
$\mathcal{P}_d^\mu$	Microwave Successful transmission probability DU's
$\mathcal{P}_c^{mm}$	Millimeter-wave Successful transmission probability CU's
$\mathcal{P}_d^{mm}$	Millimeter-wave Successful transmission probability DU's

## II. RELATED WORK

Several studies on power control in D2D communications have been conducted in the literature. The authors in [10] and [11] present a complete and tractable analytical framework for D2D-enabled uplink cellular networks with a mode selection scheme along with truncated power control. This framework is used to analyze and

understand how the underlying D2D communication affects the cellular network performance. However, the truncated power control only considers the large-scale path-loss, ignoring the small-scale fading effects, in addition, only Rayleigh fading environment is assumed, therefore, the Rician fading environment was not analyzed. In [12], the authors propose a random network model for a D2D underlaid cellular system using stochastic geometry and develops centralized and distributed power control algorithms. For the distributed power control method, the optimal on-off power control strategy is proposed, which maximizes the sum rate of the D2D links, but the power control is assumed to be some average constant. A statistical-feature-based power control, which determines the transmit power based on statistical CSI is proposed in [13]. The proposed power control combines the power control with opportunistic access control to reduce the interference caused by D2D communications and maximize the area spectral efficiency of D2D communications; however, power control is assumed to be an average constant. Using stochastic geometry, the authors in [14] evaluate the spectral efficiency and outage probability of D2D networks under generalized fading conditions assuming channel inversion-based power control. However, for power control the authors only consider the path-loss, ignoring the fading effects. Besides, the transmission power is assumed an average constant. The authors in [15] present a comprehensive framework to analyze the impact of aggregate interference from an underlay clustered D2D network on the performance of its primary cellular network, when different power control schemes are used at the D2D network, but the power control is used only at the D2D users and not at the cellular users. A channel allocation scheme together with a set of three power control schemes to mitigate interference in a D2D underlaid cellular system modeled as a random network using the mathematical tool of stochastic geometry is proposed in [16]. However, for power control the authors only consider the path-loss, ignoring the fading effects. Finally, the authors in [17] propose a location-based power control approach to mitigate the severe interference components for underlying D2D communication cellular network and the outage analysis for the cellular and D2D user is carried out by using stochastic geometry. Nevertheless, for power control the authors only consider the path-loss, ignoring the fading effects.

As we can observe, in most of these studies the transmission power of cellular and D2D users is assumed to be some average constant or only considered the large-scale pathloss, these assumptions simplify the derivation of the analytical models. In practice, the transmit power of cellular and D2D users varies due to their large-scale path-loss and small-scale fading and other factors. In this way, in our study we use power control considering both effects. Furthermore, the most important difference lies in the fact that the works [10]–[17] only consider the microwave environment, since almost all current cellular systems are deployed in the microwave bands [9]. In our work, it is considered both the microwave environment and the mm-wave environment.

In addition, we consider the channel gains to establish D2D communication, increasing the performance of the network.

On the other hand, several recent studies have also addressed the mm-wave D2D communication. In [18], the authors study the coverage and capacity of mm-wave cellular systems with a special focus on their key differentiating factors such as the limited scattering nature of mm-wave channels. However, the authors do not consider any power control. In [19] a hybrid communication model which employs mm-wave communication when there is no blockage, and switch to microwave otherwise, is proposed. Nevertheless, the authors ignore the small-scale fading in mm-wave environment and do not consider power control for microwave and mm-wave communications. The authors in [20] analyze the effect of interference cancellation in downlink mm-wave communications and exploit partial zero forcing at the user in order to cancel the interference from a set of interfering BSs and derive closed-form expression for the probability of coverage. However, the authors only study communications in mm-wave and consider the Rayleigh fading for the mm-wave environment, which is not an adequate model to characterize the channels, furthermore, power control is not considered. Aiming at the problem of aggravated interference caused by the increasing number of devices, a transmitting power optimization algorithm is proposed in [21], which combines the device association and beamwidth selection, this algorithm is based in the premise of guaranteeing the authenticity of mm-wave application scenario. Also, an mm-wave D2D network model is introduced. However, the authors do not present analytical results only results obtained by simulation, in addition to not considering power control in the developed model. In [22], the authors model the locations of cellular transmitters and receivers as homogeneous PPP and those of the D2D nodes as a Matérn cluster process, and incorporate blockages due to random objects, sectored antenna patterns, distance path-loss, and Nakagami- $m$  fading and derive closed-form expressions of the moment generating function of the aggregate interference on a D2D receiver node and its outage probability for two transmitter-receiver association schemes. Nevertheless, the authors use the truncated power control, this power control only considers the large-scale path-loss, ignoring the small-scale fading effects. An analytical framework is provided in [23] to analyze the uplink performance of D2D enabled mm-wave cellular networks with clustered D2D user equipment. The locations of cellular users are modeled as a Poisson point process, while the locations of potential D2D users are modeled as a Poisson cluster process. SINR outage probabilities are derived for both cellular and D2D links using tools from stochastic geometry. However, the authors do not consider any power control. The authors in [24] investigate the outage probability performance of a D2D communication-assisted mm-wave network by considering interference and practical hardware distortion noises. The authors do not consider the distance between the DU-TX and the DU-RX as a random variable; therefore, the model is not realistic. Finally,

in [25] the authors investigate resource allocation for D2D communication in a mm-wave cellular network where D2D users communicate in the cellular band and formulate an optimization problem of subchannel and power allocation. Nevertheless, the authors do not present analytical results only results obtained by simulation.

Unlike these studies, for our analysis we use mm-wave channel model, given by the Rician fading, based on measurements presented in [26]–[30]. Also, we presented the performance analysis for both the microwave environment and the mm-wave environment, using channel-inverse power control in both environments, thus, providing a more complete framework reference.

### III. SYSTEM MODEL

In this section, we present the system model for D2D communications underlying cellular network and the network parameters.

#### A. NETWORK MODEL

We consider a single-cell interference scenario (see Fig. 1), consisting of cellular and D2D uplinks. We assume that the inter-cell interference is managed efficiently with inter-cell interference control (ICIC) as a mechanism based on power control or resource scheduling. Therefore, we focus only on the intra-cell interference caused by the coexistence of a CU and the D2D pair. Stochastic geometry model is used to characterize the locations of the BS and users in the network. The BS position is assumed to be spatially distributed according to some independent stationary point process  $\Phi_b$  over the two-dimensional Euclidean plane, and the BS coverage area can be considered as the Poisson-Voronoi cell.

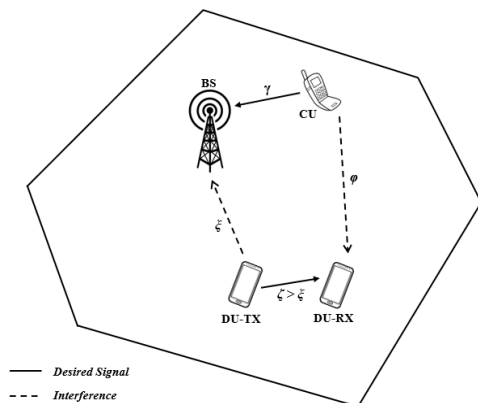


**FIGURE 1.** Network model comprises of one CU, a BS and a D2D pair. Where  $\gamma$ ,  $\xi$ ,  $\zeta$  and  $\phi$  denote the channel gains between the CU and the BS, the DU-TX and the BS, the DU-TX and the DU-RX, and from the CU to the DU-RX, respectively. Arrows indicate the direction of communication.

We assumed that the BS has only one active uplink CU scheduled. The CU are assumed to be spatially distributed as a Homogeneous Poisson Point Process (HPPP)  $\Phi_c$  with density  $\lambda_c$ , and transmission power  $P_c$ . The DUs in the network are assumed to be distributed according to a HPPP  $\Phi_d$  with density  $\lambda_d$ , and transmission power  $P_d$ . For analytical

tractability, we assume that the point processes of cellular users, D2D users and BS are independent.

On the other hand, we assume that a cellular uplink is active in the cell, in the resource assigned to cellular communication the D2D communication is established, this communication is established considering that the channel gain between the D2D transmitter (DU-TX) and the D2D receiver (DU-RX) is greater than the channel gain between DU-TX and BS. In this way, it is ensured that the D2D communication is the most adequate because the losses are lower compared to the losses that are towards the BS, taking advantage of the D2D communication benefits.

#### B. CHANNEL MODEL AND D2D ASSOCIATION

We consider small-scale multipath fading and large-scale path loss in the channel gain model. For the analysis, we assumed two small-scale fading cellular environments. The first one is a microwave environment, in which the multipath fading follows a Rayleigh fading model for both desired and interfering signal, and the large-scale path loss obeys the power law with path-loss exponent  $\alpha$ . The second one is a millimeter wave environment. In this case, we assumed that the multipath fading follows a Rician fading model with  $K$ -factor for desired signal, this assumption is based on the results presented in [26]–[30]. This model can include the line of sight (LOS) and non-line of sight (NLOS) effects, depending on the  $K$ -factor values, as shown in [26]–[30]. For the interfering channel, we assumed that the multipath fading follows a Rayleigh model. Finally, the large-scale path-loss obeys the power law with path-loss exponent  $\beta$ . All the channel gains are assumed to be independent of each other and identically distributed (i.i.d.).

It is important to consider these environments since the 5G cellular systems will be deployed in both the microwave and millimeter wave frequency bands [9].

The CU is associated with the geographically closest BS, the random distance between which is denoted by  $r$ . The random variable  $r$  can be shown to be Rayleigh distributed [31], and its probability density function (PDF) is given by (1):

$$f_c(r) = 2\pi\lambda_c r \exp(-\pi\lambda_c r^2) \quad (1)$$

We assume that the random distance  $l$  between DUs and BS also it is Rayleigh distributed and is given by (2):

$$f_d(l) = 2\pi\lambda_d l \exp(-\pi\lambda_d l^2) \quad (2)$$

#### C. CHANNEL INVERSION-BASED POWER CONTROL

The power control is an effective technique to mitigate the interference in wireless networks. In order to minimize the interference caused by the coexistence of both links (cellular and D2D) and increases network performance, we studied a Channel Inversion-Based Power Control (CIPC). In this power control scheme, the DU-TX and CU selects its transmission power,  $P_d$  and  $P_c$  respectively, based on the channel condition. This power control supposes that the receivers

have a channel state information (CSI). Under this assumption, the effects of CIPC on D2D and cellular links are studied.

Similar to [14] and [15], for microwave environment the received signal power at the BS from the CU is  $W_c^\mu = P_c h_{CU,BS} d_{CU,BS}^{-\alpha}$ , where  $d_{CU,BS}$  is the distance from the CU to the BS,  $\alpha$  is the path-loss exponent and  $h_{CU,BS}$  represents the small-scale fading. On the other hand, the receiver signal power  $W_c^\mu$  must be equal to the minimum required reception power  $P_{min}$ , i.e.,  $P_c h_{CU,BS} d_{CU,BS}^{-\alpha} = P_{min}$  and assuming CIPC the cellular transmission power is given by (3):

$$P_c = \frac{P_{min} d_{CU,BS}^\alpha}{h_{CU,BS}} \quad (3)$$

Similar to the microwave environment, for mm-wave environment, the received signal power at the BS from the CU is  $W_c^{mm} = \tilde{P}_c \tilde{h}_{CU,BS} d_{CU,BS}^{-\beta}$ , where  $\tilde{P}_c$  is the mm-wave cellular transmission power,  $\tilde{h}_{CU,BS}$  represents the small-scale fading and  $\beta$  is the path-loss exponent. Note that, the distance is the same and only changes the path-loss exponent, the small-scale fading and  $\tilde{P}_c$ . Thus, assuming CIPC and that the received signal power  $W_c^{mm}$  must be equal to the minimum required reception power  $P_{min}$ , the cellular transmission power can be expressed as (4):

$$\tilde{P}_c = \frac{P_{min} d_{CU,BS}^\beta}{\tilde{h}_{CU,BS}} \quad (4)$$

For the D2D link in microwave environment, the received signal power at the DU-RX from the DU-TX is  $W_d^\mu = P_d h_{TX,RX} d_{TX,RX}^{-\alpha}$ , where  $d_{TX,RX}$  is the distance from the DU-TX to the DU-RX and  $h_{TX,RX}$  represents the small-scale fading. Therefore, assuming CIPC and that the receiver signal power  $W_d^\mu$  must be equal to the minimum required reception power  $P_{min}$ , the D2D transmission power is given by (5):

$$P_d = \frac{P_{min} d_{TX,RX}^\alpha}{h_{TX,RX}} \quad (5)$$

In mm-wave environment, the received signal power at the DU-Rx from the DU-TX is  $W_d^{mm} = \tilde{P}_d \tilde{h}_{TX,RX} d_{TX,RX}^{-\beta}$ , where  $\tilde{P}_d$  is the mm-wave D2D transmission power,  $\tilde{h}_{TX,RX}$  represents the small-scale fading. Hence, assuming CIPC the D2D transmission power is given by (6):

$$\tilde{P}_d = \frac{P_{min} d_{TX,RX}^\beta}{\tilde{h}_{TX,RX}} \quad (6)$$

Note that this power control compensates the large-scale path-loss and small-scale fading effects, so that a minimum reception power is always ensured, increasing the network performance.

#### IV. PERFORMANCE ANALYSIS

In this section, we obtain the probability density function of the distance between users and later, using stochastic geometry we derive the cellular and D2D Successful Transmission Probability for microwave and mm-wave environment using CIPC.

#### A. DISTANCES DISTRIBUTIONS

The distance between the CU and its nearest BS follows a Rayleigh distribution. On the other hand, we need to know the probability density function of the distance between the CU and DU-RX. This PDF is given in Lemma 1.

*Lemma 1:* The probability density function of the distance  $d_{CU,RX}$  between a typical CU and a DU-RX can be expressed as (7):

$$f_{CU,RX}(x) = 2\pi\lambda_n x \exp(-\pi\lambda_n x^2), \quad \lambda_n = \frac{\lambda_c \lambda_d}{\lambda_c + \lambda_d} \quad (7)$$

*Proof:* See Appendix A.

Note that this distance also follows a Rayleigh distribution and that its parameter  $\lambda_n$  is a function of the densities of both processes.

Under the assumption that the random distance between DUs and BS is Rayleigh distributed, we must compute the probability density function of the distance between the DU-TX and DU-RX, note that they are two points of the same process, this PDF is given in Lemma 2.

*Lemma 2:* The probability density function of the distance  $d_{TX,RX}$  between the DU-TX and the DU-RX is given by (8):

$$f_{TX,RX}(y) = 2\pi\lambda_m y \exp(-\pi\lambda_m y^2), \quad \lambda_m = \frac{\lambda_d}{2} \quad (8)$$

The proof is the same that the Lemma 1. The distances  $d_{CU,RX}$  and  $d_{TX,RX}$  are illustrated in Fig. 2.

Another important probability density function for our analysis is the ratio between two distances when each follow a Rayleigh distribution. This PDF is given in Lemma 3.

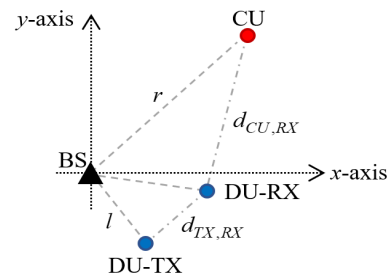


**FIGURE 2.** Illustration of the distances  $d_{CU,RX}$  and  $d_{TX,RX}$ . The BS is assumed to be located at the origin, the CU and DUs are located at  $r$  and  $l$  with respect to the BS, respectively.

*Lemma 3:* The probability density function of the ratio between two distances  $D = d_1/d_2$ , when each have a Rayleigh distribution with parameter  $\lambda_1$  and  $\lambda_2$  respectively, follow a Burr distribution [32] with parameters  $\lambda = 1/\sqrt{\Lambda}$ ,  $k = 1$  and  $c = 2$  is given by (9):

$$f_D(d) = \frac{2\Lambda d}{(\Lambda d^2 + 1)^2} \quad (9)$$

where  $\Lambda = \lambda_1/\lambda_2$ , is the density factor used in a Burr distribution.

*Proof:* See Appendix B.

**B. SIGNAL-TO-INTERFERENCE RATIO**

In this paper, we focus on the interference limited scenario since the interference is greater than the noise, i.e., the noise can be despised, and the Signal-to-Interference Ratio (SIR) is dominated.

Without loss of generality, similar to [10]–[17] we conduct the analysis on a typical cellular link that comprises a typical BS located at the origin and its associated cellular user located at a random distance  $d_{CU,BS}$  away. The received SIR at the BS in microwave environment, can be expressed as (10):

$$SIR_c^\mu = \frac{P_c h_{CU,BS} d_{CU,BS}^{-\alpha}}{P_d h_{TX,BS} d_{TX,BS}^{-\alpha}} = \left( \frac{d_{TX,BS}}{d_{TX,RX}} \right)^\alpha \frac{h_{TX,RX}}{h_{TX,BS}} \quad (10)$$

where  $P_c$  and  $P_d$  denotes the cellular and D2D power transmission using CICP given by (3) and (5) respectively,  $d_{TX,BS}$  is the distance between the DU-RX and the BS,  $d_{TX,RX}$  denotes the distance between the DU-TX and the DU-RX,  $h_{TX,RX} \sim \exp(1)$  and  $h_{TX,BS} \sim \exp(1)$  denotes the exponentially fading distribution with unit mean from the DU-TX to the DU-RX and from the DU-TX to BS respectively over the Rayleigh fading channel.

A typical D2D link comprises a D2D transmitter located at some point in the network and a D2D receiver located at a random distance  $d_{TX,RX}$  away. Shift the coordinates such that the typical D2D receiver is located at the origin. Given that the translations do not change the distribution of PPP [33], the received SIR of the typical D2D link microwave environment can be expressed as (11):

$$SIR_d^\mu = \frac{P_d h_{TX,RX} d_{TX,RX}^{-\alpha}}{P_c h_{CU,RX} d_{CU,RX}^{-\alpha}} = \left( \frac{d_{CU,RX}}{d_{CU,BS}} \right)^\alpha \frac{h_{CU,BS}}{h_{CU,RX}} \quad (11)$$

where  $d_{CU,RX}$  is the distance between the CU and the D2D receiver,  $d_{CU,BS}$  denotes the distance between the CU and the BS,  $h_{CU,RX} \sim \exp(1)$  and  $h_{CU,BS} \sim \exp(1)$  denote the exponentially fading distribution with unit mean from the CU to the DU-RX from the CU to BS respectively.

Like the microwave environment, the received SIR at the BS in mm-wave environment is given by (12):

$$SIR_c^{mm} = \frac{\tilde{P}_c \tilde{h}_{CU,BS} d_{CU,BS}^{-\beta}}{\tilde{P}_d \tilde{h}_{TX,BS} d_{TX,BS}^{-\beta}} = \left( \frac{d_{TX,BS}}{d_{TX,RX}} \right)^\beta \frac{\tilde{h}_{TX,RX}}{\tilde{h}_{TX,BS}} \quad (12)$$

where  $\tilde{P}_c$  and  $\tilde{P}_d$  denotes the cellular and D2D power transmission using CICP for mm-wave channels given by (4) and (6) respectively and  $\tilde{h}_{TX,BS} \sim \exp(1)$  denotes the exponentially distributed fading power with unit mean from the DU-TX to BS (interfering link) over the Rayleigh fading channel. Due that the desired link between the DU-TX and the DU-RX experience the Rician fading, hence the PDF of  $\tilde{h}_{TX,RX}$  is given at [34] by (13):

$$f_{\tilde{h}_{TX,RX}}(h) = \exp(-K_d - h) I_0(\sqrt{4K_d h}) \quad (13)$$

where  $I_0(\cdot)$  is the zeroth order modified Bessel function of the first kind, and  $K_d$  is the Rician fading parameter that is defined as the ratio between the amplitude of the dominant

path and the variance of the weak paths. On the other hand, the received SIR of the typical D2D link mm-wave environment can be expressed as (14):

$$SIR_d^{mm} = \frac{\tilde{P}_d \tilde{h}_{TX,RX} d_{TX,RX}^{-\beta}}{\tilde{P}_c \tilde{h}_{CU,RX} d_{CU,RX}^{-\beta}} = \left( \frac{d_{CU,RX}}{d_{CU,BS}} \right)^\beta \frac{\tilde{h}_{CU,BS}}{\tilde{h}_{CU,RX}} \quad (14)$$

where  $\tilde{h}_{CU,RX} \sim \exp(1)$  denotes the exponentially distributed fading power from the CU to DU-RX over the Rayleigh fading channel, and for the desired link from CU to BS, the PDF of  $\tilde{h}_{CU,BS}$  is given by (15):

$$f_{\tilde{h}_{CU,BS}}(h) = \exp(-K_c - h) I_0(\sqrt{4K_c h}) \quad (15)$$

where  $K_c$  is the Rician fading parameter for cellular link. Note that (13) and (15) are used to obtain the cellular and D2D successful transmission probability in the mm-wave environment (see Appendix D).

**C. MICROWAVE SUCCESSFUL TRANSMISSION PROBABILITY**

The successful transmission probability is defined as the probability that the SIR exceeds a threshold  $T$ , i.e.  $\mathcal{P} = P(SIR > T)$ , equivalently to the CCDF of SIR.

The cellular successful transmission probability in microwave environment is defined as (16):

$$\mathcal{P}_c^\mu = P\left( \left( \frac{d_{TX,BS}}{d_{TX,RX}} \right)^\alpha \frac{h_{TX,RX}}{h_{TX,BS}} > T \mid \frac{h_{TX,RX}}{d_{TX,RX}^\alpha} > \frac{h_{TX,BS}}{d_{TX,BS}^\alpha} \right) \quad (16)$$

Applying some algebra over (16) we obtain (17):

$$\mathcal{P}_c^\mu = P(h_{TX,RX} > T h_{TX,BS} D_c^\alpha \mid h_{TX,RX} > h_{TX,BS} D_c^\alpha) \quad (17)$$

where  $D_c = d_{TX,RX}/d_{TX,BS}$  and follows the PDF with parameter  $\Lambda_c = \lambda_n/\lambda_d$  given in lemma 3, expression (9).

The condition is due to the fact that D2D communication is established considering that the channel conditions between the DU-TX and the DU-RX are greater that the channel conditions between the DU-TX and BS. In this way, it is ensured that the D2D communication is the most adequate since the losses are lower compared to the losses that are towards the BS. The D2D successful transmission probability is defined as (18):

$$\mathcal{P}_d^\mu = P\left( \left( \frac{d_{CU,RX}}{d_{CU,BS}} \right)^\alpha \frac{h_{CU,BS}}{h_{CU,RX}} > T \mid \frac{h_{TX,RX}}{d_{TX,RX}^\alpha} > \frac{h_{TX,BS}}{d_{TX,BS}^\alpha} \right) \quad (18)$$

Note that the condition is independent of the SIR, therefore the successful transmission probability is given by (19):

$$\mathcal{P}_d^\mu = P(h_{CU,BS} > T h_{CU,RX} D_d^\alpha) \quad (19)$$

where  $D_d = d_{CU,BS}/d_{CU,RX}$  and follows the distribution with parameter  $\Lambda_d = \lambda_c/\lambda_m$  given by lemma 3, expression (9).

The cellular and D2D successful transmission probabilities in microwave environment are given in the following theorems.

*Theorem 1:* For CIPC in microwave environment, the cellular successful transmission probability is given by (20):

$$\mathcal{P}_c^\mu = \frac{\rho(\Lambda_c, \alpha, \max\{1, T\})}{\rho(\Lambda_c, \alpha, 1)} \quad (20)$$

*Theorem 2:* For CIPC in microwave environment, the successful transmission probability for D2D user can be expressed as (21):

$$\mathcal{P}_d^\mu = \rho(\Lambda_d, \alpha, T) \quad (21)$$

where  $\rho(\Lambda, \alpha, T)$  is given by (22):

$$\rho(\Lambda, \alpha, T) = \int_0^\infty \frac{2\Lambda u}{(\Lambda u^2 + 1)^2 (Tu^\alpha + 1)} du \quad (22)$$

*Proof:* See Appendix C.

#### D. MILLIMETER-WAVE SUCCESSFUL TRANSMISSION PROBABILITY

Like to the microwave environment, the cellular successful transmission probability in mm-wave environment is defined as (23):

$$\mathcal{P}_c^{mm} = \mathbb{P}\left(\tilde{h}_{TX,RX} > T\tilde{h}_{TX,BS}D_c^\beta \mid \tilde{h}_{TX,RX} > \tilde{h}_{TX,BS}D_c^\beta\right) \quad (23)$$

Remembering that the condition is independent of the SIR, therefore the D2D successful probability in mm-wave environment is given by (24):

$$\mathcal{P}_d^{mm} = \mathbb{P}\left(\tilde{h}_{CU,BS} > T\tilde{h}_{CU,RX}D_d^\beta\right) \quad (24)$$

Note that the distances ratio distribution is the same regardless of the environment. The cellular and D2D successful transmission probabilities in mm-wave environment are given in the following theorem 3 and theorem 4, respectively.

*Theorem 3:* In mm-wave environment, the successful transmission probability of the cellular uplink using CIPC is given by (25):

$$\mathcal{P}_c^{mm} = \frac{\zeta(\Lambda_c, \beta, K_c, \max\{1, T\})}{\zeta(\Lambda_c, \beta, K_c, 1)} \quad (25)$$

*Theorem 4:* In mm-wave environment, the D2D successful transmission probability can be calculated as (26):

$$\mathcal{P}_d^{mm} = \zeta(\Lambda_d, \beta, K_d, T) \quad (26)$$

where  $\zeta(\Lambda, \beta, K, T)$  is given by (27):

$$\zeta(\Lambda, \beta, K, T) = 1 - 2\Lambda \int_0^\infty \frac{Tv^{\beta+1}}{(\Lambda v^2 + 1)^2 (Tv^\beta + 1)} \times \exp\left(-\frac{K}{Tv^\beta + 1}\right) dv \quad (27)$$

*Proof:* See Appendix D.

*Corollary 1:* For high value of  $T$ , the expression of  $\zeta(\Lambda, \beta, K, T)$  can be approximated as (28):

$$\zeta(\Lambda, \beta, K, T) \approx 1 - \int_0^\infty \frac{2\Lambda v}{(\Lambda v^2 + 1)^2} \exp\left(-\frac{K}{Tv^\beta}\right) dv \quad (28)$$

*Proof:* Given large values of  $T$  we have that  $1 + Tv^\beta \rightarrow Tv^\beta$ , therefore  $(Tv^{\beta+1})/(1 + Tv^\beta)$  is reduced to only  $v$ , and in this way, we obtain Corollary 1.

Using Corollary 1, we can obtain closed-form results of special cases for path-loss exponent values.

#### E. SPECIAL CASES

In the case of  $\alpha = 2$ ,  $\rho(\Lambda, \alpha, T)$  for the successful transmission probability for cellular and D2D users for microwave environment is given by (29):

$$\rho(\Lambda, 2, T) = \frac{\Lambda(\Lambda + T(\ln(T/\Lambda) - 1))}{(\Lambda - T)^2} \quad (29)$$

And for  $\alpha = 4$  which is widely used for wireless systems,  $\rho(\Lambda, \alpha, T)$  for Microwave environment can be expressed as (30):

$$\rho(\Lambda, 4, T) = \frac{\Lambda}{2(\Lambda^2 + T)^2} \times \left(2\Lambda^3 - \pi\sqrt{T}\Lambda^2 + \pi T^{\frac{3}{2}} + 2T\Lambda(\ln(\Lambda^2/T) + 1)\right) \quad (30)$$

In the mm-wave channel models for 5G wireless networks described in [35]–[37], it was showed that some environments have values of path-loss exponent  $\beta$  between 2 and 4. Some of these environments include indoor, urban microcell, suburban macrocell and given the nature of D2D communications, line-of-sight conditions can be experienced. For path loss exponent  $\beta = 2$ ,  $\zeta(\Lambda, \beta, K, T)$  for the successful transmission probability for cellular and D2D users for mm-wave environment is given by (31):

$$\zeta(\Lambda, 2, K, T) = \frac{\Lambda K}{T} \exp\left(\frac{\Lambda K}{T}\right) \Gamma\left(0, \frac{\Lambda K}{T}\right) \quad (31)$$

where  $\Gamma(a, x)$  is the incomplete gamma function defined by  $\Gamma(a, x) = \int_x^\infty t^{a-1} \exp(-t) dt$ . And for path loss exponent  $\beta = 4$  the function  $\zeta(\Lambda, \beta, K, T)$  is given by (32):

$$\zeta(\Lambda, 4, K, T) = \sqrt{\pi\eta} - \eta \exp(-\eta) \times [\pi \operatorname{Erfi}(\sqrt{\eta}) - \operatorname{Ei}(\eta)] \quad (32)$$

where  $\operatorname{Erfi}(x)$  is the imaginary error function and  $\operatorname{Ei}(x)$  is the exponential integral defined by  $\operatorname{Ei}(x) = \int_{-\infty}^x t^{-1} \exp(t) dt$ , and  $\eta = \Lambda^2 K/T$ .

It is noted that the derived successful transmission probabilities analytical expressions are simple and depending only on the densities factors, the SIR threshold, and the Rician  $K$ -factor (for mm-wave environment).

V. NUMERICAL RESULTS AND DISCUSSION

In this section, we validate the analytical results and evaluate the performance of our proposed system model through numerical simulation. We provide some numerical results to compare analytical results with simulation results. To justify analytical results, the simulations with  $1 \times 10^5$  realizations are performed to plot the successful transmission probability of cellular and D2D users for microwave and mm-wave environment for different system metrics such as, path loss exponents, densities users and Rician factors. The system parameters used are summarized in table 2.

For the results presented in this section, specifically fig. 3 and fig. 4, we can observe that the analytical results closely match with the corresponding simulation results, which validates our analysis.

TABLE 2. System parameters.

Density of cellular users $\lambda_c$	$2 \times 10^{-5} m^{-2}$
Density of D2D users $\lambda_d$	$2 \times 10^{-5} m^{-2}$
Microwave path-loss exponent $\alpha$	2, 4
Millimeter-wave path-loss exponent $\beta$ [34]	2, 4
Rician factor $K_c$ [28]	11 dB
Rician factor $K_d$ [28]	15 dB
Minimum reception power $P_{min}$	-30 dBm
SIR threshold $T$	-20 dBm to 20 dBm

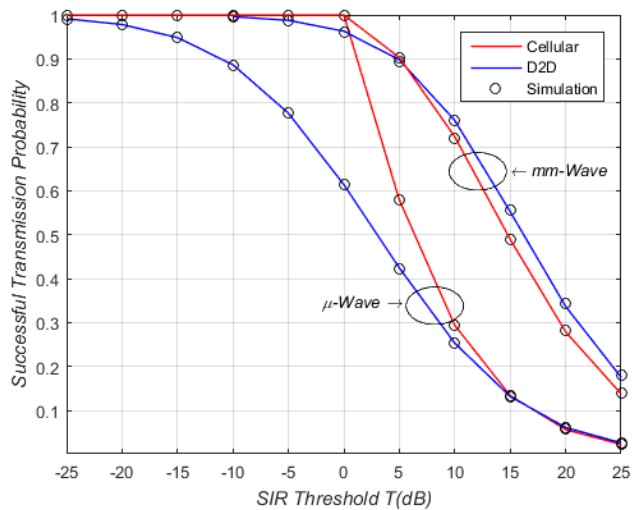


FIGURE 3. Cellular and D2D Successful Transmission Probability in microwave and mm-wave environment for  $\alpha = 2$ .

In Fig. 3 and 4 we present the cellular and D2D successful transmission probability in microwave and mm-wave environment for  $\alpha = 2$  and  $\alpha = 4$ , respectively.

We can show that mm-wave environment achieves higher successful transmission probability than microwave environment. This is because, given the channel properties, the interference in mm-wave is much smaller compared with microwave environment when a strong dominant path

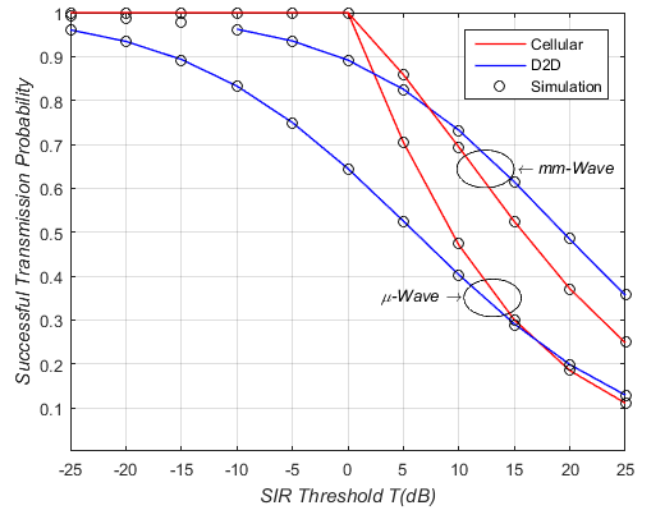


FIGURE 4. Cellular and D2D Successful Transmission Probability in microwave and mm-wave environment for  $\alpha = 4$ .

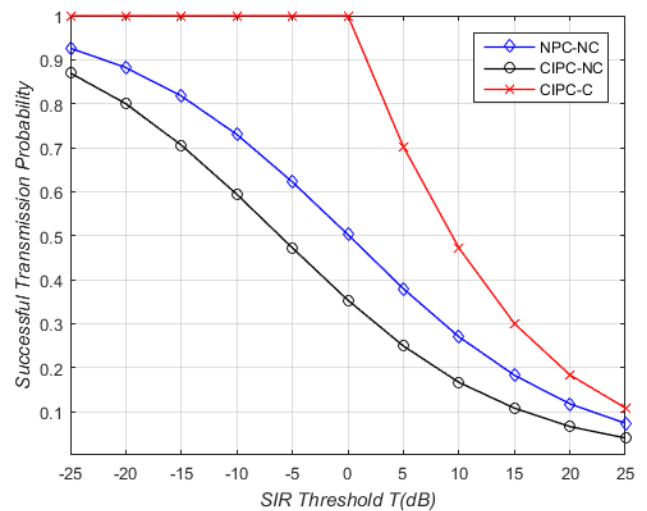


FIGURE 5. Cellular Successful Transmission Probability comparison in microwave environment between NPC-NC, CIPC-NC, and CIPC-C.

exists between the desired receiver and transmitter. So, that interfering signals affect to a lesser extent having a weak amplitude. Also, given the existence of a dominant component for LOS or NLOS environments, the desired received signal is stronger.

Fig. 5 shows the cellular successful transmission probability in microwave environment when power control is not used and no condition is considered to establish D2D communication (NPC-NC), when CIPC is used as a power control but no condition is considered to establish D2D communication (CIPC-NC) and when CIPC is used and a channel gain condition is considered to establish D2D communication (CIPC-C). We can observe that CIPC-C presents better performance with a successful transmission probability of 100% compared to 35% for NPC-NC when  $T = 0$  dB, provide a network performance improvement. Note that for CIPC-C the D2D communication are established considering the best



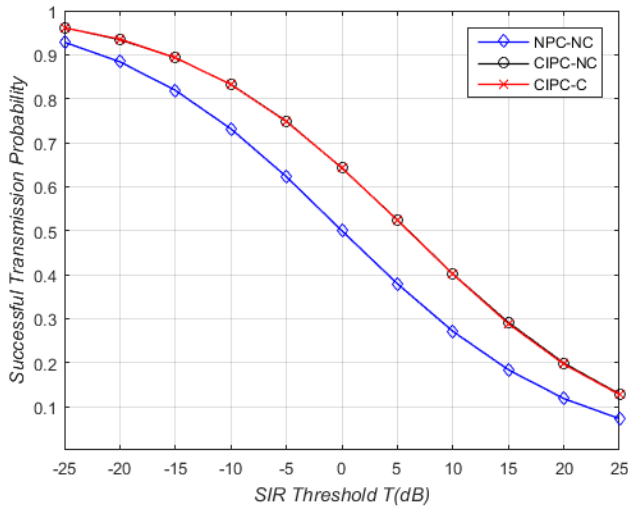


FIGURE 6. D2D Successful Transmission Probability comparison in microwave environment between NPC-NC, CIPC-NC, and CIPC-C.

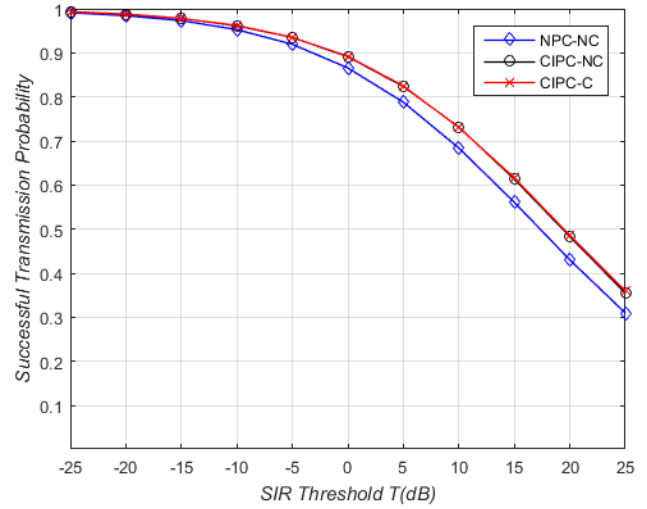


FIGURE 8. D2D Successful Transmission Probability comparison in mm-wave environment between NPC-NC, CIPC-NC, and CIPC-C.

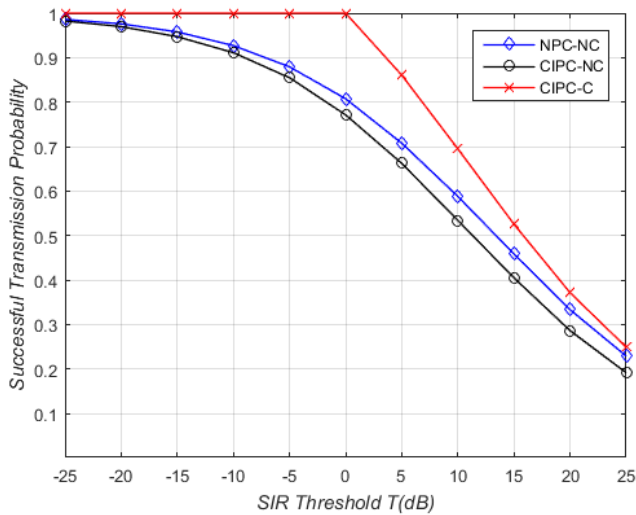


FIGURE 7. Cellular Successful Transmission Probability comparison in mm-wave environment between NPC-NC, CIPC-NC, and CIPC-C.

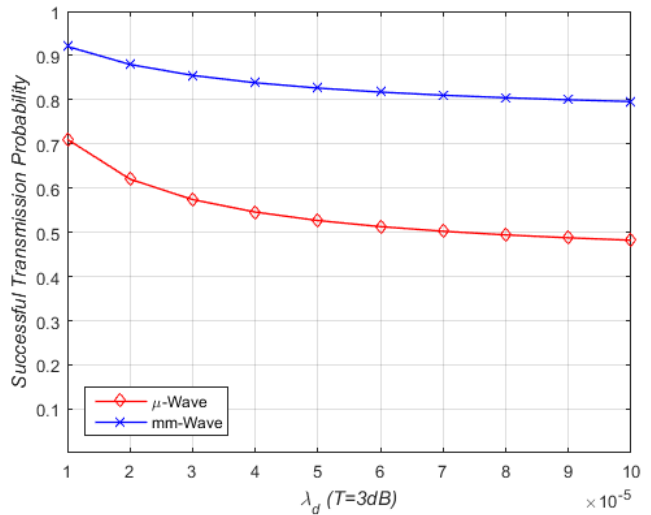


FIGURE 9. Successful Transmission Probability vs. the D2D density  $\lambda_d$  for microwave and mm-wave environment.

channel between DU-TX and DU-RX respect DU-TX and BS so the interference is reduced in the cellular link.

Fig. 6 shows the successful transmission probability for D2D link in microwave environment for NPC-NC, CIPC-NC, and CIPC-C. As can be observed, due to the power control, CIPC-NC and CIPC-C have the same performance and can provide more than 30% performance improvement for the network respect to NPC-NC. On the other hand, Fig. 7 shows the cellular successful transmission probability in mm-wave environment. We can observe that in mm-wave the cellular link has better performance respect to microwave environment, besides CIPC-C presents better performance than other cases, providing an improvement of about 28%.

For D2D communication in mm-wave environment, in Fig. 8 we can see that the same effect occurs as in the microwave environment, due to the power control, the

performance is the same when it is conditioned and when the D2D communication is not conditioned.

Fig. 9 shows the impact in the D2D successful transmission probability for microwave and mm-wave environment of different D2D density users. We can see that increasing DUs density leads to a decrease in the successful transmission probability, clearly, when the density of users increases, the proximity of users produces more interference, degrading the network performance.

Finally, as the Fig. 10 shows, the cellular and D2D successful transmission probability under Rician fading for mm-wave environments increases with the fading parameter  $K$  and is always larger than under Rayleigh fading (microwave environment). So, if when we have large  $K$ -factors the amplitude of the dominant path is much higher than the variance of the weak paths. Thus, the  $K$ -factor impact becomes more important.

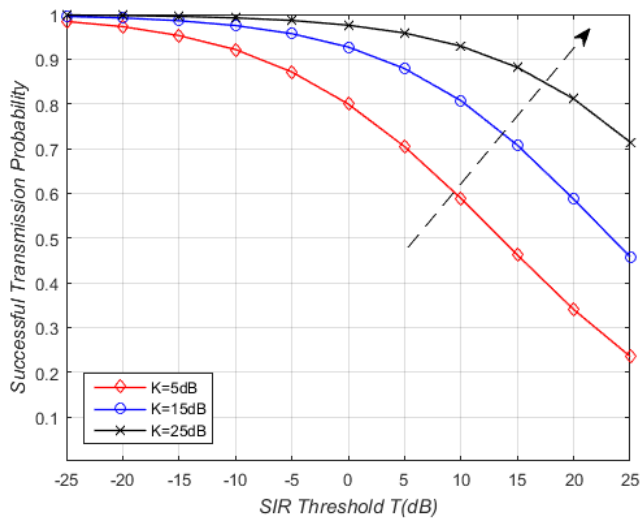


FIGURE 10. Successful Transmission Probability for different factors under CIPC.

VI. CONCLUSION

In this paper, we investigated the performance of D2D communication using power control in microwave and millimeter-wave cellular networks considering the underlay mode of operation. Two different environments have been investigated, the microwave environment, where the Rayleigh model is assumed to describe the multipath fading, and the millimeter-wave environment, where it is assumed that the multipath fading follows a Rician model. On the other hand, we propose a channel gain-based condition to establish the D2D link, where the D2D communication is carried out considering the channel gain between transmitter and receiver to establish the D2D link. Also, we assume the channel inversion-based power control as a strategy to mitigate the intra-cell interference and increase the network performance. Moreover, using the stochastic geometry tools, we derived the successful transmission probability for cellular and D2D links in both microwave and millimeter-wave environments.

The performance gains are validated by analytical and numerical results. The results show that the proposed model presents better performance when a channel gain-based condition is considered to carry out the D2D communication and the power control is used to mitigate the interference. Moreover, we observe that the mm-wave environment presents better performance than the microwave environment, due to its channel characteristics. Future work could investigate, inter-cell interference, other power control techniques and the effect of multiple antennas and beams at the base station and devices.

APPENDIX

A. PROOF OF LEMMAS 1 AND 2

The Fig. 2 illustrates the considered setting to obtain the distance between two points (CU and DU-RX) of different point processes, we assume that the BS is located at the origin, the point of the processes  $\Phi_1$  is located at  $(x_1, y_1)$  with

distance to the origin  $d_{o,1}$  where its PDF is characterized by Rayleigh distribution given by (33):

$$f_{d_{o,1}}(r_1) = 2\pi\lambda_1 r_1 \exp(-\pi\lambda_1 r_1^2) \tag{33}$$

On the other hand, the point of the processes  $\Phi_2$  is located at  $(x_2, y_2)$  with distance to the origin  $d_{o,2}$  with PDF characterized by Rayleigh distribution given by (34):

$$f_{d_{o,2}}(r_2) = 2\pi\lambda_2 r_2 \exp(-\pi\lambda_2 r_2^2) \tag{34}$$

Besides, let  $d_{1,2}$  be the distance between both points. Therefore, the distance  $d_{1,2}$  can be obtained as (35):

$$d_{1,2} = \sqrt{(x_2 - x_1)^2 + (y_2 - y_1)^2} \tag{35}$$

where  $x_1$  and  $x_2$  follow a PDF with parameters  $\lambda_1$  and  $\lambda_2$  respectively given by (36):

$$f_X(x) \stackrel{(a)}{=} \sqrt{\lambda} \exp(-\pi\lambda x^2) \sim N_X\left(\mu_X = 0, \sigma_X = \frac{1}{\sqrt{2\pi\lambda}}\right) \tag{36}$$

where (a) is obtained for the transformation  $x = r \cos(\theta)$  when  $\theta$  is uniformly distributed between  $-\pi$  and  $\pi$ ,  $r$  follows a Rayleigh distribution, and  $N_X(\mu_X, \sigma_X)$  is the normal distribution with parameters  $\mu_X$  and  $\sigma_X$ .

On the other hand,  $y_1$  and  $y_2$  also follow a Normal distribution with parameters  $\lambda_1$  and  $\lambda_2$  respectively, this as a result of the transformation  $y = r \sin(\theta)$  when  $-\pi < \theta < \pi$  is uniformly distributed,  $r$  follows a Rayleigh distribution, and is given by (37):

$$f_Y(y) = \sqrt{\lambda} \exp(-\pi\lambda y^2) \sim N_Y\left(\mu_Y = 0, \sigma_Y = \frac{1}{\sqrt{2\pi\lambda}}\right) \tag{37}$$

Derived from the properties of the normal distribution, we have that the difference  $x = x_1 - x_2$  between two random variables normally distributed also follows a Normal distribution given by (38):

$$\begin{aligned} f_X(x) &\sim N_X(\mu_{X_2} - \mu_{X_1}, \sigma_{X_2}^2 + \sigma_{X_1}^2) \\ &\sim N_X\left(\mu_X = 0, \sigma_X = \sqrt{\frac{2\pi\lambda_2 + 2\pi\lambda_1}{(2\pi)^2 \lambda_2 \lambda_1}}\right) \\ &\sim N_X\left(\mu_X = 0, \sigma_X = \frac{1}{\sqrt{2\pi\lambda_e}}\right) \end{aligned} \tag{38}$$

where  $\lambda_e = (\lambda_1\lambda_2)/(\lambda_1 + \lambda_2)$ . The difference  $y = y_2 - y_1$  also follows a Normal distribution given by (39):

$$f_Y(y) \sim N_Y\left(\mu_Y = 0, \sigma_Y = \frac{1}{\sqrt{2\pi\lambda_e}}\right) \tag{39}$$

Finally, the distance  $d_{1,2}$  between both points can be obtained as (40):

$$d_{1,2} = \sqrt{x^2 + y^2} \stackrel{(b)}{\sim} Rayleigh\left(\sigma = \frac{1}{\sqrt{2\pi\lambda_{eq}}}\right) \tag{40}$$

where (b) is obtained by the fact that the sum of two squared random variables with Normal distribution with same parameter  $\sigma$  and mean zero follows a Rayleigh distribution. When both points belong to the same point process, the framework to obtain the distance is the same with the difference that  $\lambda = \lambda_1 = \lambda_2$  and  $\lambda_e = \lambda/2$ . Note that when  $\lambda_1 = \lambda_c$  and  $\lambda_2 = \lambda_d$  we have (7) and when  $\lambda = \lambda_d$  we have (8).

**B. PROOF OF LEMMA 3**

Let  $x$  and  $y$  be two random variables with Rayleigh distribution each one with parameters  $\lambda_1$  and  $\lambda_2$  respectively, and the ratio  $z = x/y$  between two random variables can be obtained as (41):

$$f_Z(z) = \int_0^\infty w f_X(zw) f_Y(w) dw \tag{41}$$

Therefore, when  $x$  and  $y$  follow a Rayleigh distribution, and by (35) the ratio is given as (42):

$$f_Z(z) = \lambda_1 \lambda_2 (2\pi)^2 z \int_0^\infty w^3 \exp(-\pi w^2 (z^2 \lambda_1 + \lambda_2)) dw \tag{42}$$

By a change of variable  $t = \pi w^2 (z^2 \lambda_1 + \lambda_2)$  we have:

$$f_Z(z) = \frac{2\lambda_1 \lambda_2 z}{(z^2 \lambda_1 + \lambda_2)^2} \int_0^\infty t \exp(-t) dt \tag{43}$$

$$\stackrel{(a)}{=} \frac{2\lambda_1 \lambda_2 z}{(z^2 \lambda_1 + \lambda_2)^2} \stackrel{(b)}{=} \frac{2\Lambda z}{(\Lambda z^2 + 1)^2}$$

where (a) follows with the definition of the gamma function  $\int_{-\infty}^x t \exp(-t) dt = \Gamma(2) = 1$ ; (b) follows by divide the numerator and denominator by  $\lambda_2^2$  and change  $\Lambda = \lambda_1/\lambda_2$  and applying some algebra we completed the proof.

**C. PROOF OF THEOREMS 1 AND 2**

The successful transmission probability for a typical cellular user in microwave environment given in theorem 1 can be calculated as follows:

$$\mathcal{P}_c^\mu = \mathbb{P}(h_{TX,RX} > Th_{TX,BS} D_c^\alpha | h_{TX,RX} > h_{TX,BS} D_c^\alpha)$$

The condition in the successful transmission probability is since the channel conditions are considered to establish D2D communication. Using Bayes' rule, we have:

$$\mathcal{P}_c^\mu = \frac{\mathbb{P}(h_{TX,RX} > Th_{TX,BS} D_c^\alpha, h_{TX,RX} > h_{TX,BS} D_c^\alpha)}{\mathbb{P}(h_{TX,RX} > h_{TX,BS} D_c^\alpha)}$$

$$\stackrel{(a)}{=} \frac{\mathbb{P}(h_{TX,RX} > h_{TX,BS} D_c^\alpha \max(1, T))}{\mathbb{P}(h_{TX,RX} > h_{TX,BS} D_c^\alpha)}$$

where (a) is obtained for the intersection of both events. Due that  $h_{TX,RX}$  and  $h_{TX,BS}$  are i.i.d. and exponentially distributed with unit mean, we can see that the probability for numerator and denominator are the same with the only change of factor  $\max(1, T)$  that is a constant. First,

we focus on the terms in the numerator and we can write it as follows:

$$\mathbb{P}(h_{TX,RX} > h_{TX,BS} D_c^\alpha t)$$

$$= \int_0^\infty \int_0^\infty \int_{h_{TX,BS} D_c^\alpha t}^\infty f_{TX,RX}(x) f_{TX,BS}(y) f_{D_c}(z) dx dy dz$$

$$\stackrel{(a)}{=} \int_0^\infty \int_0^\infty \left[ \int_{yz^\alpha t}^\infty \exp(-x) dx \right] \exp(-y) \frac{2\Lambda z}{(\Lambda z^2 + 1)^2} dy dz$$

$$\stackrel{(b)}{=} \int_0^\infty \left[ \int_0^\infty \exp(-y(z^\alpha t + 1)) dy \right] \frac{2\Lambda z}{(\Lambda z^2 + 1)^2} dz$$

$$\stackrel{(c)}{=} \int_0^\infty \frac{1}{(z^\alpha t + 1)} \frac{2\Lambda z}{(\Lambda z^2 + 1)^2} dz \tag{44}$$

where  $t = \max(1, T)$ , (a) follows from substituting the PDF of  $h_{TX,RX}$ ,  $h_{TX,BS}$  and  $D_c$  in the integral and by changing the variable  $h_{TX,RX} = x$ ,  $h_{TX,BS} = y$ ,  $D_c = z$ , (b) is obtained by solving the integral over  $x$  and evaluating, (c) is obtained by applying some algebra and solving the integral over  $y$  and evaluating at the integration limits. For denominator is the same framework only changing  $t$  by 1 and is given by (45):

$$\mathbb{P}(h_{TX,RX} > h_{TX,BS} D_c^\alpha) = \int_0^\infty \frac{1}{(z^2 + 1)} \frac{2\Lambda z}{(\Lambda z^2 + 1)^2} dz \tag{45}$$

On the other hand, the successful transmission probability for a typical D2D receiver in microwave environment given in theorem 2 can be calculated as:

$$\mathcal{P}_d^\mu = \mathbb{P}(h_{CU,BS} > Th_{CU,RX} D_d^\alpha)$$

$$= \int_0^\infty \int_0^\infty \int_{h_{TX,BS} D_c^\alpha T}^\infty f_{TX,RX}(x) f_{TX,BS}(y) f_{D_c}(z) dx dy dz$$

$$\stackrel{(a)}{=} \int_0^\infty \frac{1}{(z^2 T + 1)} \frac{2\Lambda z}{(\Lambda z^2 + 1)^2} dz = \rho(\Lambda, \lambda, T) \tag{46}$$

where (a) is obtained following the same framework used to obtain (44). Note that (44) and (45) can be expressed like (46) as follows  $\rho(\Lambda, \alpha, \max(1, T))$  and  $\rho(\Lambda, \alpha, 1)$ , respectively.

**D. PROOF OF THEOREMS 3 AND 4**

The cellular successful transmission probability in mm-wave environment given in (25) can be obtained as follows:

$$\mathcal{P}_c^{mm} = \mathbb{P}(\tilde{h}_{TX,RX} > T\tilde{h}_{TX,BS} D_c^\beta | \tilde{h}_{TX,RX} > \tilde{h}_{TX,BS} D_c^\beta)$$

Like microwave environment, the condition is due to the fact the D2D communication is established considering the channel conditions. Using Bayes' rule, we have:

$$\mathcal{P}_c^{mm} = \frac{\mathbb{P}(\tilde{h}_{TX,RX} > T\tilde{h}_{TX,BS} D_c^\beta, \tilde{h}_{TX,RX} > \tilde{h}_{TX,BS} D_c^\beta)}{\mathbb{P}(\tilde{h}_{TX,RX} > \tilde{h}_{TX,BS} D_c^\beta)}$$

$$= \frac{\mathbb{P}(\tilde{h}_{TX,RX} > \tilde{h}_{TX,BS} D_c^\beta \max(1, T))}{\mathbb{P}(\tilde{h}_{TX,RX} > \tilde{h}_{TX,BS} D_c^\beta)}$$

where  $\tilde{h}_{TX,BS}$  is exponentially distributed with unit mean,  $\tilde{h}_{TX,RX}$  is distributed with PDF given by (13) when we model the channel as Rician fading channel, therefore for the numerator we have:

$$\begin{aligned}
 & P\left(\tilde{h}_{TX,RX} > \tilde{h}_{TX,BS} D_c^\beta\right) \\
 &= \int_0^\infty \int_0^\infty \int_{\tilde{h}_{TX,BS} D_c^\beta}^\infty f_{\tilde{h}_{TX,RX}}(x) f_{\tilde{h}_{TX,BS}}(y) f_{D_c}(z) dx dy dz \\
 &\stackrel{(a)}{=} \int_0^\infty \int_0^\infty \left[ \int_{yz^\beta w}^\infty e^{-K_d x} I_0(\sqrt{4K_d x}) dx \right] e^{-y} f_{D_c}(z) dy dz \\
 &\stackrel{(b)}{=} \int_0^\infty f_{D_c}(z) \int_0^\infty e^{-y} \sum_{m=0}^\infty \frac{e^{-K_d} K_d^m}{m! \Gamma(m+1)} \int_{yz^\beta w}^\infty x^m e^{-x} dx dy dz \\
 &\stackrel{(c)}{=} \int_0^\infty f_{D_c}(z) \int_0^\infty e^{-y} \sum_{m=0}^\infty \frac{e^{-K_d} K_d^m}{m! m!} \Gamma(m+1, yz^\beta w) dy dz \\
 &\stackrel{(d)}{=} \int_0^\infty f_{D_c}(z) \int_0^\infty e^{-y} \sum_{m=0}^\infty \frac{e^{-K_d} K_d^m m!}{m! m!} e^{-yz^\beta w} \\
 &\quad \times \sum_{n=0}^m \frac{(yz^\beta w)^n}{n!} dy dz \\
 &= \int_0^\infty f_{D_c}(z) \sum_{m=0}^\infty \frac{e^{-K_d} K_d^m}{m!} \sum_{n=0}^m \frac{(z^\beta w)^n}{n!} \\
 &\quad \times \int_0^\infty y^n e^{-y(z^\beta w + 1)} dy dz \\
 &\stackrel{(e)}{=} \int_0^\infty f_{D_c}(z) \sum_{m=0}^\infty \frac{e^{-K_d} K_d^m}{m!} \sum_{n=0}^m \frac{(z^\beta w)^n}{(z^\beta w + 1)^{n+1}} dz \\
 &\stackrel{(f)}{=} \int_0^\infty f_{D_c}(z) \sum_{m=0}^\infty \frac{e^{-K_d} K_d^m}{m!} \left[ 1 - \left( \frac{z^\beta w}{z^\beta w + 1} \right)^{m+1} \right] dz \\
 &\stackrel{(g)}{=} 1 - \int_0^\infty \frac{2\Lambda z}{(\Lambda z^2 + 1)^2} \frac{z^\beta w}{z^\beta w + 1} \exp\left(\frac{-K_d}{z^\beta w + 1}\right) dz \quad (47)
 \end{aligned}$$

where  $w = \max(1, T)$ , (a) follows from substituting the PDF of  $\tilde{h}_{TX,RX}$ ,  $\tilde{h}_{TX,BS}$  and  $D_c$  in the integral and by change of variable  $\tilde{h}_{TX,RX} = x$ ,  $\tilde{h}_{TX,BS} = y$ ,  $D_c = z$ , (b) is obtained by expanding  $I_0(\sqrt{4K_d x})$  into infinite series according to [38, 8.350], (c) is obtained because the inner integral can be changed into gamma incomplete function  $\Gamma(a, x)$  given in [39, 8.350.2], (d) is derived by expand  $\Gamma(a, x)$  into infinite series following [39, 8.352.2] and substituting  $\Gamma(m+1) = m!$ , (e) is obtained by integrating each term in  $y$ , (f) is derived summing the series in  $n$ , finally (g) is obtained applying some algebra, summing the series in  $m$  and substituting the PDF of  $D_c$ . For denominator is the same procedure only changing  $w$  by 1 and is given by (48):

$$\begin{aligned}
 & P\left(\tilde{h}_{TX,RX} > \tilde{h}_{TX,BS} D_c^\beta\right) \\
 &= 1 - \int_0^\infty \frac{2\Lambda z}{(\Lambda z^2 + 1)^2} \frac{z^\beta}{z^\beta + 1} \exp\left(\frac{-K_d}{z^\beta + 1}\right) dz \quad (48)
 \end{aligned}$$

On the other hand, the successful transmission probability for a typical D2D receiver in mm-wave environment given

in (26) can be obtained following the same framework used to obtain (47) with  $w = T$  and changing  $K_d$  by  $K_c$  when  $\tilde{h}_{CU,BS}$  is distributed with PDF given by (15), therefore can be expressed as (49):

$$\begin{aligned}
 \mathcal{P}_d^{mm} &= P\left(\tilde{h}_{CU,BS} > T \tilde{h}_{CU,RX} D_d^\beta\right) \\
 &= \int_0^\infty \int_0^\infty \int_{\tilde{h}_{TX,BS} D_c^\beta T}^\infty f_{\tilde{h}_{TX,RX}}(x) f_{\tilde{h}_{TX,BS}}(y) f_{D_c}(z) dx dy dz \\
 &= 1 - \int_0^\infty \frac{2\Lambda z}{(\Lambda z^2 + 1)^2} \frac{z^\beta T}{(z^\beta T + 1)} \exp\left(\frac{-K_c}{z^\beta T + 1}\right) dz \quad (49)
 \end{aligned}$$

For corollary 1 we apply the approximation for high SIR regimen where for large values of  $T$  we have that  $1 + Tv^\beta \rightarrow Tv^\beta$ , therefore  $(Tv^{\beta+1})/(1 + Tv^\beta) = v$ , then (49) can be approximating by (50):

$$\mathcal{P}_d^{mm} \approx 1 - 2\Lambda \int_0^\infty \frac{z}{(\Lambda z^2 + 1)^2} \exp\left(\frac{-K_c}{Tz^\beta}\right) dv \quad (50)$$

Note that (49) is the function  $\zeta(\Lambda, \beta, K, T)$ , thus (47) can be expressed like (49) for high SIR approximation as follows  $\zeta(\Lambda, \beta, K, \max(1, T))$  and  $\zeta(\Lambda, \beta, K, 1)$ .

## REFERENCES

- [1] S. K. Sharma, I. Woungang, A. Anpalagan, and S. Chatzinotas, "Toward tactile Internet in beyond 5G era: Recent advances, current issues, and future directions," *IEEE Access*, vol. 8, pp. 56948–56991, Mar. 2020.
- [2] M. Masoudi et al., "Green mobile networks for 5G and beyond," *IEEE Access*, vol. 7, pp. 107270–107299, Aug. 2019.
- [3] J. Iqbal, M. A. Iqbal, A. Ahmad, M. Khan, A. Qamar, and K. Han, "Comparison of spectral efficiency techniques in device-to-device communication for 5G," *IEEE Access*, vol. 7, pp. 57440–57449, May 2019.
- [4] D. Chatzopoulos, C. Bermejo, E. Haq, Y. Li, and P. Hui, "D2D task offloading: A dataset-based Q&A," *IEEE Commun. Mag.*, vol. 57, no. 2, pp. 102–107, Feb. 2019.
- [5] R. I. Ansari, C. Chrysostomou, S. A. Hassan, M. Guizani, S. Mumtaz, J. Rodriguez, and J. J. P. C. Rodrigues, "5G D2D networks: Techniques, challenges, and future prospects," *IEEE Syst. J.*, vol. 12, no. 4, pp. 3970–3984, Dec. 2018.
- [6] Y. Yang, Y. Zhang, L. Dai, J. Li, S. Mumtaz, and J. Rodriguez, "Transmission capacity analysis of relay-assisted device-to-device overlay/underlay communication," *IEEE Trans. Ind. Informat.*, vol. 13, no. 1, pp. 380–389, Feb. 2017.
- [7] J. Huang, C.-C. Xing, and M. Guizani, "Power allocation for D2D communications with SWIPT," *IEEE Trans. Wireless Commun.*, vol. 19, no. 4, pp. 2308–2320, Apr. 2020.
- [8] L. Zhang, H. Zhao, S. Hou, Z. Zhao, H. Xu, X. Wu, Q. Wu, and R. Zhang, "A survey on 5G millimeter wave communications for UAV-assisted wireless networks," *IEEE Access*, vol. 7, pp. 117460–117504, Jul. 2019.
- [9] M. Shafi, J. Zhang, H. Tataria, A. F. Molisch, S. Sun, T. S. Rappaport, F. Tufvesson, S. Wu, and K. Kitao, "Microwave vs. millimeter-wave propagation channels: Key differences and impact on 5G cellular systems," *IEEE Commun. Mag.*, vol. 56, no. 12, pp. 14–20, Dec. 2018.
- [10] H. El Sawy, E. Hossain, and M.-S. Alouini, "Analytical modeling of mode selection and power control for underlay D2D communication in cellular networks," *IEEE Trans. Commun.*, vol. 62, no. 11, pp. 4147–4161, Nov. 2014.
- [11] K. S. Ali, H. El Sawy, and M.-S. Alouini, "On mode selection and power control for uplink D2D communication in cellular networks," in *Proc. IEEE Int. Conf. Commun. Workshop (ICCW)*, Jun. 2015, pp. 620–626.
- [12] N. Lee, X. Lin, J. G. Andrews, and R. W. Heath, Jr., "Power control for D2D underlaid cellular networks: Modeling, algorithms, and analysis," *IEEE J. Sel. Areas Commun.*, vol. 33, no. 1, pp. 1–13, Jan. 2015.
- [13] P. Sun, K. G. Shin, H. Zhang, and L. He, "Transmit power control for D2D-underlaid cellular networks based on statistical features," *IEEE Trans. Veh. Technol.*, vol. 66, no. 5, pp. 4110–4119, May 2017.

- [14] Y. J. Chun, S. L. Cotton, H. S. Dhillon, A. Ghayeb, and M. O. Hasna, "A stochastic geometric analysis of device-to-device communications operating over generalized fading channels," *IEEE Trans. Wireless Commun.*, vol. 16, no. 7, pp. 4151–4165, Jul. 2017.
- [15] T. Illandara, K. T. Hemachandra, and T. Samarasinghe, "On the coverage probability of cellular networks with underlaid clustered device-to-device networks using power control," in *Proc. IEEE Int. Conf. Adv. Netw. Telecommun. Syst. (ANTS)*, Dec. 2017, pp. 1–6.
- [16] A. Abdallah, M. M. Mansour, and A. Chehab, "Power control and channel allocation for D2D underlaid cellular networks," *IEEE Trans. Commun.*, vol. 66, no. 7, pp. 3217–3234, Jul. 2018.
- [17] P. Pawar, A. Trivedi, and M. K. Mishra, "Outage and ASE analyses for power controlled D2D communication," *IEEE Syst. J.*, vol. 14, no. 2, pp. 2269–2280, Jun. 2020.
- [18] S. Akoum, O. El Ayach, and R. W. Heath, "Coverage and capacity in mmWave cellular systems," in *Proc. Conf. Rec. 46th Asilomar Conf. Signals, Syst. Comput. (ASILOMAR)*, Nov. 2012, pp. 688–692.
- [19] F. Wang, H. Wang, H. Feng, and X. Xu, "A hybrid communication model of millimeter wave and microwave in D2D network," in *Proc. IEEE 83rd Veh. Technol. Conf. (VTC Spring)*, May 2016, pp. 1–5.
- [20] A. H. Jafari, J. Park, and R. W. Heath, Jr., "Analysis of interference mitigation in mmWave communications," in *Proc. IEEE Int. Conf. Commun. (ICC)*, May 2017, pp. 1–6.
- [21] Z. Zhang, C. Wang, H. Yu, M. Wang, and S. Sun, "Power optimization assisted interference management for D2D communications in mmWave networks," *IEEE Access*, vol. 6, pp. 50674–50682, Sep. 2018.
- [22] S. Kusaladharma, Z. Zhang, and C. Tellambura, "Interference and outage analysis of random D2D networks underlying millimeter-wave cellular networks," *IEEE Trans. Commun.*, vol. 67, no. 1, pp. 778–790, Jan. 2019.
- [23] E. Turgut and M. C. Gursoy, "Uplink performance analysis in D2D-enabled millimeter-wave cellular networks with clustered users," *IEEE Trans. Wireless Commun.*, vol. 18, no. 2, pp. 1085–1100, Feb. 2019.
- [24] L. Tlebaldiyeva, B. Maham, and T. A. Tsiftsis, "Device-to-device mmWave communication in the presence of interference and hardware distortion noises," *IEEE Commun. Lett.*, vol. 23, no. 9, pp. 1607–1610, Sep. 2019.
- [25] S. G. Hong, J. Park, and S. Bahk, "Subchannel and power allocation for D2D communication in mmWave cellular networks," *J. Commun. Netw.*, vol. 22, no. 2, pp. 118–129, Apr. 2020.
- [26] M. K. Samimi and T. S. Rappaport, "3-D millimeter-wave statistical channel model for 5G wireless system design," *IEEE Trans. Microw. Theory Techn.*, vol. 64, no. 7, pp. 2207–2225, Jul. 2016.
- [27] M. K. Samimi, G. R. MacCartney, S. Sun, and T. S. Rappaport, "28 GHz millimeter-wave ultrawideband small-scale fading models in wireless channels," in *Proc. IEEE 83rd Veh. Technol. Conf. (VTC Spring)*, May 2016, pp. 1–6.
- [28] D. Dupleich, N. Iqbal, C. Schneider, S. Häfner, R. Müller, S. Skoblikov, J. Luo, G. D. Galdo, and R. Thomä, "Influence of system aspects on fading at mm-waves," *IET Microw., Antennas Propag.*, vol. 12, no. 4, pp. 516–524, Mar. 2018.
- [29] D. Dupleich, N. Iqbal, C. Schneider, S. Häfner, R. Müller, S. Skoblikov, J. Luo, and R. Thoma, "Investigations on fading scaling with bandwidth and directivity at 60 GHz," in *Proc. 11th Eur. Conf. Antennas Propag. (EUCAP)*, Mar. 2017, pp. 1–5.
- [30] N. Iqbal, C. Schneider, J. Luo, D. Dupleich, R. Müller, S. Häfner, and R. S. Thoma, "On the stochastic and deterministic behavior of mmWave channels," in *Proc. 11th Eur. Conf. Antennas Propag. (EUCAP)*, Mar. 2017, pp. 1–5.
- [31] T. D. Novlan, H. S. Dhillon, and J. G. Andrews, "Analytical modeling of uplink cellular networks," *IEEE Trans. Wireless Commun.*, vol. 12, no. 6, pp. 2669–2679, Jun. 2013.
- [32] P. R. Tadikamalla, "A look at the burr and related distributions," *Int. Stat. Rev.*, vol. 43, no. 3, pp. 337–344, Dec. 1980.
- [33] C. Ma, W. Wu, Y. Cui, and X. Wang, "On the performance of successive interference cancellation in D2D-enabled cellular networks," in *Proc. IEEE Conf. Comput. Commun. (INFOCOM)*, Apr. 2015, pp. 37–45.
- [34] A. Goldsmith, *Wireless Communications*. Cambridge, U.K.: Cambridge Univ. Press, Aug. 2005.
- [35] A. I. Sulyman, A. T. Nassar, M. K. Samimi, G. R. Maccartney, T. S. Rappaport, and A. Alsanie, "Radio propagation path loss models for 5G cellular networks in the 28 GHz and 38 GHz millimeter-wave bands," *IEEE Commun. Mag.*, vol. 52, no. 9, pp. 78–86, Sep. 2014.
- [36] S. Sun, T. S. Rappaport, T. A. Thomas, A. Ghosh, H. C. Nguyen, I. Z. Kovacs, I. Rodriguez, O. Koymen, and A. Partyka, "Investigation of prediction accuracy, sensitivity, and parameter stability of large-scale propagation path loss models for 5G wireless communications," *IEEE Trans. Veh. Technol.*, vol. 65, no. 5, pp. 2843–2860, May 2016.
- [37] P. Zhang, B. Yang, C. Yi, H. Wang, and X. You, "Measurement-based 5G millimeter-wave propagation characterization in vegetated suburban macrocell environments," *IEEE Trans. Antennas Propag.*, vol. 68, no. 7, pp. 5556–5567, Jul. 2020.
- [38] M. Abramowitz and I. A. Stegun, *Handbook of Mathematical Functions With Formulas, Graphs, and Mathematical Tables*, 9th ed. New York, NY, USA: Dover, Nov. 1970.
- [39] I. S. Gradshteyn and I. M. Ryzhik, *Table of Integrals, Series, and Products*, 7th ed. New York, NY, USA: Academic, 2007.



degree.

His main research interests include, but is not limited to, performance evaluation, interference analysis in cellular networks, device-to-device communications, 5G, microwave and millimeter-wave cellular networks, energy efficiency, propagations analysis, and antenna design and characterization.



**DOMINGO LARA-RODRÍGUEZ** received the M.Sc. and Ph.D. degrees in electrical engineering from the Center for Research and Advance Studies, National Polytechnic Institute of Mexico (IPN), Mexico. He is currently with the Center for Research Advanced Studies, Mobile Telecommunications Research Group, IPN. His main research interest includes performance modeling of mobile cellular networks. He has published extensively in this area in international conferences and journals.

• • •